

MetaMixer: A Regularization Strategy for Online Knowledge Distillation

Maorong Wang, Ling Xiao, Toshihiko Yamasaki

The University of Tokyo

{ma_wang, ling, yamasaki}@cvm.t.u-tokyo.ac.jp

Abstract

Online knowledge distillation (KD) has received increasing attention in recent years. However, while most existing online KD methods focus on developing complicated model structures and training strategies to improve the distillation of high-level knowledge like probability distribution, the effects of the multi-level knowledge in the online KD are greatly overlooked, especially the low-level knowledge. Thus, to provide a novel viewpoint to online KD, we propose MetaMixer, a regularization strategy that can strengthen the distillation by combining the low-level knowledge that impacts the localization capability of the networks, and high-level knowledge that focuses on the whole image. Experiments under different conditions show that MetaMixer can achieve significant performance gains over state-of-the-art methods.

1. Introduction

In recent years, we have witnessed the success of deep neural networks in various computer vision tasks [17, 10, 6, 22, 9, 46]. The success of deep learning has been largely driven by ever-larger models [29, 10]. However, whilst training large models helps to improve the performance, deploying those cumbersome deep models is challenging due to the high computational overhead of such models and their large memory footprint. To address this problem, compression techniques have been investigated. The existing model compression meta-solution can be mainly classified into network pruning [20, 25, 36], lightweight structure design [14, 21], parameter quantization [8, 35], and knowledge distillation (KD) [13], etc.

As one of the most successful model compression schemes, knowledge distillation (KD) has been proposed and proven to have a strong ability to train a compact student network by mimicking the probability distribution (also known as “soft targets”) generated by a high-capacity pre-trained teacher network. This process allows the student network to learn the “dark knowledge” [13, 39] from the teacher network and achieve superior performance com-

pared to training independently from scratch.

After the conventional KD was proposed, there are many works to improve the performance of the student network [28, 3, 45, 24, 11, 12, 41]. However, in the conventional KD framework, the teacher model is pre-trained and fixed, and the knowledge can only be transferred from the teacher to the student. Additionally, the high-capacity pre-trained teacher is not always available, which further limits the applicability of the conventional KD method. To fill the gap, online distillation is proposed [44, 18, 2], which trains a set of student networks from scratch in a peer-teaching manner. Surprisingly, student networks trained using online distillation methods have shown the potential to compete with, and in some cases, even outperform networks trained with a strong pre-trained teacher network [44].

However, while most existing collaborative learning methods focus on designing more complex training graphs and using auxiliary branches to improve the distillation of the *high-level* dark knowledge like probability distributions and feature embeddings from the feature extractors [44, 7, 4, 19, 18, 37], the importance of knowledge from low-level features is greatly underestimated. To this end, we propose MetaMixer, a regularization strategy that can boost the transfer of multi-level knowledge, including both low-level knowledge that contains localizable features and high-level knowledge that are more abstract and focuses on the whole image.

Our main contributions are listed as follows:

- (1) We proposed MetaMixer, a regularization method for online knowledge distillation.
- (2) We stressed the importance of low-level knowledge in online KD, and we proposed a distillation strategy that can take advantage of dark knowledge with different levels of abstraction.
- (3) We evaluated MetaMixer on multiple benchmark datasets and network structures and verified our higher performance over the state-of-the-art online KD methods.

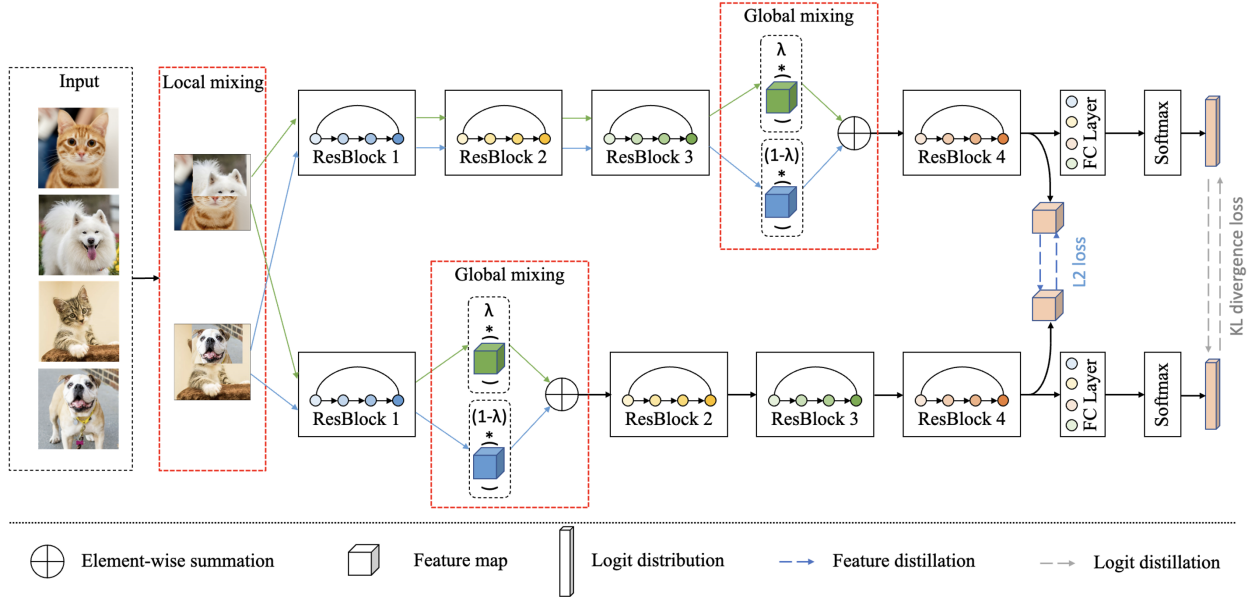


Figure 1: This figure shows a two-student online KD scheme equipped with the proposed MetaMixer. MetaMixer uses a two-stage mixing strategy consisting of local mixing and global mixing, allowing an organized mixing of four different images from two random classes. The local mixing aims to foster localizable low-level knowledge among students and is implemented prior to image input. In contrast, the global mixing encourages knowledge transferring from different levels of abstraction and can happen at any stage of feature extraction (E.g. Prior to any residual block of ResNet networks).

2. Related Work

2.1. Conventional Knowledge Distillation

The idea of transferring dark knowledge from the high-capacity teacher model to the compact student model was first proposed in [1]. However, it did not gain significant attention from researchers until the work by Hinton et al. [13], where the Kullback-Leibler (KL) divergence loss is used to minimize the difference between the probability distribution generated by a student network and the soft targets generated by a pre-trained teacher network. Besides the vanilla KD, researchers have explored more methods to extract more salient dark knowledge from the pre-trained teacher network to the student [28, 15, 26, 27, 31, 30]. For example, Fitnets [28] proposed to use intermediate feature representation as a hint to guide the training of the student network. Tian et al. [30] first used the contrastive learning mechanism to extract the structural knowledge of the teacher network to supervise the training of the student.

2.2. Online Knowledge Distillation

Whilst the success of conventional KD, its two-stage training process can be time-consuming. Also, the high-performance teacher model may not always be available, which limits the conventional KD in some practical scenarios.

To address the problem, online knowledge distillation was proposed. Deep mutual learning [44] first proposed to train a set of student networks in a peer-teaching manner, showing that online KD methods can train student networks that are competitive with ones trained with conventional KD methods. ONE [18] firstly applied ensemble learning strategy into online distillation. In ONE, multiple auxiliary branches are applied to the networks. By incorporating auxiliary classifiers and a gate controller, predictions from all branches can be integrated to create a powerful soft target that guides the training of each branch. AFD [4] extracted the knowledge from the intermediate feature representations and used an adversarial training mechanism to further improve the performance of online KD. TSB [19] proposed temporal accumulators which can stabilize the training process by incorporating predictions during the training procedure. KDCL [7] added distortions to the training samples of student networks and designed several effective methods to generate the soft targets containing more dark knowledge. MCL [38] first introduced the contrastive learning mechanism to the field of online distillation.

2.3. Image Mixture

Image mixture has been a successful data augmentation strategy to improve the robustness and generalization ability of neural networks. It involves combining multiple images into a single image, which can help the network learn more robust features. There are several ways to perform image mixture, such as random cropping, random erasing, and random masking. In this work, we propose a two-stage mixing strategy consisting of local mixing and global mixing, allowing an organized mixing of four different images from two random classes. The local mixing aims to foster localizable low-level knowledge among students and is implemented prior to image input. In contrast, the global mixing encourages knowledge transferring from different levels of abstraction and can happen at any stage of feature extraction (E.g. Prior to any residual block of ResNet networks).

ity of deep networks. Mixup [43] casts a pixel-level interpolation between two images and a linear interpolation of training labels. CutMix [40] performs a patch-level mixture which can further improve the localization ability of networks. Manifold Mixup [33] applied interpolations in the intermediate feature representations. In the field of knowledge distillation, Wang et al. [34] use Mixup to augment the training data to achieve a data-efficient distillation. However, all of the existing image mixture techniques are one-step mixing, and none of the previous research explores the two-step mixing technique in the field of knowledge distillation.

3. The Proposed Method

In this section, we present the overall process of our proposed MetaMixer. As shown in Fig. 1, MetaMixer combines the knowledge of different scales and boosts the knowledge transfer with two mixing stages. For the sake of simplicity, we elaborate the proposed method with two student networks. We will also discuss the generalization to multiple student networks later in this section.

3.1. MetaMixing

We abstract our mixing procedure in MetaMixer as MetaMixing, which consists of two stages: **local mixing** and **global mixing**.

Local mixing is the first stage of the mixing process in our proposed MetaMixing. As shown in Fig. 1, given four samples $c_1, c_2 \in \mathcal{C}$ and $d_1, d_2 \in \mathcal{D}$ (\mathcal{C} and \mathcal{D} denote two random classes), their local mixing and label, denoted as (m_1, y_1) and (m_2, y_2) , can be expressed as:

$$\begin{aligned} m_1 &= M \odot c_1 + (1 - M) \odot d_1, \\ m_2 &= M \odot c_2 + (1 - M) \odot d_2, \\ \{y_1, y_2\} &= \lambda_1 \cdot y_c + (1 - \lambda_1) \cdot y_d, \end{aligned} \quad (1)$$

where λ_1 is the combination ratio sampled from a beta distribution $Beta(\alpha_1, \alpha_1)$ and \odot is an element-wise multiplication. $M \in \{0, 1\}^{W \times H}$ is a rectangular binary mask with a width of $\sqrt{\lambda_1} \cdot W$ and a height of $\sqrt{\lambda_1} \cdot H$, and the location of the mask M is randomly selected for every local mixing operation. It has been proved that this kind of patch-based mixing operation is a robust regularization strategy to train networks with a strong localization capability [40]. And we claim that local mixing is helpful in transferring local-aware low-level knowledge between student peers and improving the localization capability of student networks.

Global mixing is the second stage of MetaMixing implemented in the feature space of networks, as illustrated in Fig. 1. Consider a neural network $f(x) = FC(f_k(g_k(x)))$ consists of a feature extractor $f_k(g_k(\cdot))$ and a linear classifier $FC(\cdot)$, where $g_k(\cdot)$ denotes the first k layers of the network which map the input to the hidden representation at

the layer k , and $f_k(\cdot)$ denotes the rest part of the feature extractor mapping the hidden representation $g_k(x)$ to the final feature.

Given two random inputs from local mixing $\{m_1, m_2\}$, we can produce a global mixing of feature representation $\tilde{g}_k(m_1, m_2)$ at the k -th layer:

$$\tilde{g}_k(m_1, m_2) = \lambda_2 \cdot g_k(m_1) + (1 - \lambda_2) \cdot g_k(m_2), \quad (2)$$

where λ_2 is the mixing coefficient of a beta distribution $Beta(\alpha_2, \alpha_2)$. Global mixing encourages the student network to transfer knowledge from different levels for an online KD scheme.

With local mixing and global mixing, the MetaMixer can effectively extract and transfer dark knowledge of different scales between student peers through its two-stage mixing operation and improve the learning ability of the whole model.

3.2. Formulation of Training Graph

In our description, we refer to the network being supervised as the student network, while we name the other networks that guide the training of the student network as the peer-teacher network(s). For online distillation, in a training iteration, the role of the student network and the peer-teacher network is interchanging. For simplicity, we will introduce the loss function with two student networks in detail, and the method can be easily generalized to more networks and will be discussed later in this section.

Consider an online KD scheme with two networks. We use f^s to denote the student network that is being trained and f^t to denote the peer-teacher network that guides the training of the student network. For either the student network or the peer-teacher network $f^{(\cdot)}$, the forward pass with MetaMixer can be expressed as:

$$\tilde{f}^{(\cdot)}(m_1, m_2) = FC^{(\cdot)}(f_k^{(\cdot)}(\tilde{g}_k^{(\cdot)}(m_1, m_2))), \quad (3)$$

where layer k of global mixing is individually randomly selected with each forward pass.

In each training iteration, the role of f^s and f^t is not fixed, and every network in the student cohort is assigned to f^s for once. The supervision of f^s can be expressed as follows.

Classification loss. In our work, we use cross-entropy as the classification loss. Specifically, for the input $\{(c_1, y_c), (c_2, y_c), (d_1, y_d), (d_2, y_d)\}$ and their local mixing $\{(m_1, y_1), (m_2, y_2)\}$, the loss of student network f^s can be expressed as:

$$\mathcal{L}_{cls}^s = \sum_{i=1}^2 (l_{cls}^s(c_i, y_c) + l_{cls}^s(d_i, y_d) + l_{cls}^s(m_i, y_i)), \quad (4)$$

where $l_{cls}^s(x, y) = \mathcal{L}_{CE}(\sigma(f^s(x)), y)$, $\sigma(\cdot)$ is the softmax function to normalize the logits to probability distributions, and $\mathcal{L}_{CE}(\cdot)$ is the cross-entropy loss.

Logit KD loss with MetaMixing. As the soft target of the teacher network is often regarded as a probability distribution that contains dark knowledge [13], we encourage the student network to behave linearly in the logit distribution between the soft targets of the teacher model. Thus, the linear interpolation of feature maps at any depth k (the depth may include 0) should lead to the corresponding linear interpolation of the final probability distributions with the same interpolation proportion. Similar to other KD works, we use Kullback-Leibler (KL) divergence to minimize the difference between the soft targets and the probability distribution generated by the student network.

Given two inputs $\{m_1, m_2\}$, the logit-based distillation loss for student network f^s can be expressed as:

$$\mathcal{L}_{m_logit}^s = \mathcal{T}^2 \|\sigma(\tilde{f}^s(m_1, m_2)/\mathcal{T}), \sigma(\tilde{f}^t(m_1, m_2)/\mathcal{T})\|_{KL}, \quad (5)$$

where \mathcal{T} is the temperature parameter and $\|\cdot\|_{KL}$ stands for KL divergence.

Feature map KD loss. Beyond the logit distribution, the feature maps often contain valuable knowledge from the models. Similar to the logit distribution, we also encourage the student network to behave consistently in the feature domain. Inspired by FitNet [28], we also use the l_2 norm to minimize the difference between the feature maps. Also, to reduce the computational cost, as shown in Fig. 1, we only use the feature map from the last layer of the feature extractor.

For two inputs $\{m_1, m_2\}$ from local mixing, the feature level distillation loss of student network f^s can be expressed as:

$$\mathcal{L}_{fea}^s = \frac{1}{HWC} \|f_k^s(\tilde{g}_k^s(m_1, m_2)), f_k^t(\tilde{g}_k^t(m_1, m_2))\|_2, \quad (6)$$

where $\|\cdot\|_2$ is the l_2 norm, and H , W , and C are the height, width, and number of channels of the feature maps.

In our work, since the student network f^s and peer-teacher network f^t are not necessarily identical, there is a case where the feature embeddings of f^s and f^t are of different shapes. Under such conditions, we linearly interpolate the feature embeddings of the peer-teacher network to the shape of the student network to achieve the feature map distillation.

Logit KD loss without global mixing. While the MetaMixer actively regularizes the probability distribution of samples interpolated between m_1 and m_2 , it is also important to regularize the interpolation endpoints m_1 and m_2 . Thus, we employ a logit distillation on the interpolation endpoints (m_1, y_1) and (m_2, y_2) . Moreover, we apply a weight factor \mathcal{W} as a confidence score to guide the distillation process. We measure the confidence of peer models by calculating the cross-entropy of the predictions and the

ground truth on the training dataset and give more weight to the student models with a higher confidence score. The confidence score \mathcal{W}_i^1 of the student network f^s on sample (m_i, y_i) can be calculated as:

$$\mathcal{W}_i^s = \frac{l_{cls}^t(m_i, y_i)}{l_{cls}^s(m_i, y_i) + l_{cls}^t(m_i, y_i)}, \quad (7)$$

where $l_{cls}(\cdot)$ is the cross-entropy loss between sample m_i and label y_i . Moreover, the confidence scores are detached from the training graph to prevent models from collapsing. With the confidence score \mathcal{W} , the distillation loss of student network f^s can be expressed as:

$$\begin{aligned} \mathcal{L}_{e_logit}^s = & \mathcal{T}^2 \mathcal{W}_1^s \cdot \|\sigma(f^s(m_1)/\mathcal{T}), \sigma(f^t(m_1)/\mathcal{T})\|_{KL} + \\ & \mathcal{T}^2 \mathcal{W}_2^s \cdot \|\sigma(f^s(m_2)/\mathcal{T}), \sigma(f^t(m_2)/\mathcal{T})\|_{KL}, \end{aligned} \quad (8)$$

where \mathcal{T} is the same temperature parameter as in Eq. 5.

In summary, the overall loss function of the student network f^s can be expressed as:

$$\mathcal{L}^s = \mathcal{L}_{cls}^s + \beta \mathcal{L}_{m_logit}^s + \gamma \mathcal{L}_{fea}^s + \delta \mathcal{L}_{e_logit}^s, \quad (9)$$

where β, γ, δ are balancing hyperparameters. With our hyperparameter search, we find that $\beta = 4, \delta = 2$ gives the best performance. For the value of γ , we find that the $\gamma \in (10^{-1}, 10^{-2})$ functions well, and we set the $\gamma = 4 \times 10^{-2}$ to make the magnitude of feature l_2 loss comparable with other loss terms.

Generalize to multiple student networks. The generalization of our method to more student networks is quite straightforward, and it can be regarded as ensembling peer-teacher networks into a single stronger peer-teacher network by averaging the predictions and feature embedding of peer-teacher networks. For example, consider a distillation with n networks, which can be denoted as a student network f^s and $n - 1$ peer-teacher networks $\{f^{t1}, f^{t2}, \dots, f^{t(n-1)}\}$. We can ensemble all peer-teacher networks f^{ti} into a single strong peer-teacher network f^t by:

$$\begin{aligned} \tilde{f}^t(x_1, x_2) &= \frac{1}{n-1} \sum_{i=1}^{n-1} \tilde{f}^{ti}(x_1, x_2), \\ f_k^t(\tilde{g}_k^t(m_1, m_2)) &= \frac{1}{n-1} \sum_{i=1}^{n-1} f_k^{ti}(\tilde{g}_k^{ti}(m_1, m_2)), \end{aligned} \quad (10)$$

and apply the strong peer-teacher network f^t to the loss functions above.

4. Experiments and Results

4.1. Experimental Setup

In this section, we evaluate our proposed method with benchmark network structures including ResNet [10], Wide

| Network | Baseline | DML | | ONE | | KDCL | | MCL | | MetaMixer (Ours) | |
|-------------------------|----------|-------|-------|-------|-------|-------|-------|-------|-------|------------------|--------------|
| | | Avg. | Ens. | Avg. | Ens. | Avg. | Ens. | Avg. | Ens. | Avg. | Ens. |
| ResNet-32 | 93.46 | 93.85 | 94.31 | 94.04 | 94.11 | 93.67 | 94.28 | 94.13 | 94.74 | 94.92 | 95.37 |
| ResNet-56 | 94.08 | 94.25 | 94.80 | 94.72 | 95.01 | 94.35 | 94.86 | 94.62 | 95.06 | 95.63 | 96.09 |
| ResNet-110 | 94.47 | 94.61 | 95.00 | 95.14 | 95.45 | 94.39 | 94.93 | 94.86 | 95.37 | 96.07 | 96.44 |
| WRN-16-2 | 93.79 | 94.14 | 94.51 | 94.35 | 94.74 | 94.45 | 94.66 | 94.27 | 94.59 | 95.27 | 95.56 |
| WRN-40-2 | 95.07 | 95.08 | 95.58 | 95.61 | 96.02 | 95.22 | 95.73 | 95.27 | 95.65 | 96.60 | 96.92 |
| VGG-13-BN | 94.23 | 94.63 | 95.09 | 94.74 | 95.07 | 94.60 | 95.05 | 94.68 | 95.11 | 95.57 | 95.94 |
| ShuffleNetV2 $\times 1$ | 92.29 | 93.41 | 94.00 | 93.28 | 93.73 | 93.84 | 94.40 | 93.07 | 93.61 | 93.96 | 94.55 |

| Network | Baseline | DML | | ONE | | KDCL | | MCL | | MetaMixer (Ours) | |
|-------------------------|----------|-------|-------|-------|-------|-------|-------|-------|-------|------------------|--------------|
| | | Avg. | Ens. | Avg. | Ens. | Avg. | Ens. | Avg. | Ens. | Avg. | Ens. |
| ResNet-32 | 71.10 | 72.64 | 74.60 | 72.67 | 74.51 | 72.58 | 74.87 | 72.70 | 75.23 | 74.79 | 76.45 |
| ResNet-56 | 72.88 | 74.13 | 75.99 | 76.51 | 77.23 | 74.86 | 76.43 | 74.49 | 77.25 | 76.93 | 78.70 |
| ResNet-110 | 74.14 | 75.42 | 77.10 | 77.97 | 78.51 | 75.76 | 77.72 | 76.20 | 78.26 | 78.58 | 80.50 |
| WRN-16-2 | 72.96 | 74.07 | 75.68 | 74.05 | 75.04 | 75.18 | 76.90 | 74.51 | 76.73 | 76.40 | 77.88 |
| WRN-40-2 | 75.87 | 77.35 | 79.15 | 79.04 | 80.23 | 78.02 | 79.85 | 77.55 | 79.69 | 80.18 | 81.91 |
| VGG-13-BN | 74.08 | 75.74 | 77.12 | 75.93 | 77.06 | 77.01 | 78.50 | 77.02 | 78.42 | 78.28 | 79.47 |
| ShuffleNetV2 $\times 1$ | 72.52 | 74.66 | 76.34 | 74.31 | 75.57 | 74.84 | 77.20 | 73.21 | 75.84 | 76.96 | 78.20 |

Table 1: Top-1 test accuracy (%) compared with various online distillation methods on CIFAR-10 (top) and CIFAR-100 (bottom) dataset by training two networks with the same architecture. The baseline refers to the performance of the network when it is trained independently with only cross-entropy loss. Due to the special configuration of ONE, we regard the different branches as different networks. The *Avg.* denotes the average performance of the models and *Ens.* refers to the ensemble performance of two networks. Reported the average performance of three runs.

| Network | | Baseline | | DML | | | KDCL | | | MetaMixer (Ours) | | |
|-----------|------------|----------|-------|-------|-------|-------|-------|-------|-------|------------------|--------------|--------------|
| Net 1 | Net 2 | Net 1 | Net 2 | Net 1 | Net 2 | Ens. | Net 1 | Net 2 | Ens. | Net 1 | Net 2 | Ens. |
| ResNet-20 | ResNet-32 | 92.76 | 93.46 | 92.91 | 93.50 | 93.87 | 93.16 | 93.82 | 94.04 | 94.16 | 94.96 | 95.24 |
| ResNet-56 | ResNet-110 | 94.08 | 94.47 | 94.39 | 94.88 | 95.14 | 94.24 | 94.49 | 94.90 | 95.76 | 96.19 | 96.40 |
| ResNet-32 | WRN-16-2 | 93.46 | 93.79 | 93.74 | 94.15 | 94.58 | 94.21 | 94.55 | 94.81 | 95.14 | 95.17 | 95.59 |
| WRN-16-2 | WRN-28-2 | 93.79 | 94.94 | 94.47 | 95.05 | 95.27 | 94.61 | 95.43 | 95.63 | 95.27 | 96.23 | 96.29 |
| WRN-16-2 | WRN-40-2 | 93.79 | 95.15 | 94.33 | 95.27 | 95.30 | 94.53 | 95.55 | 95.78 | 95.31 | 96.54 | 96.44 |
| VGG-13-BN | WRN-16-2 | 94.23 | 93.79 | 94.57 | 94.15 | 95.03 | 94.70 | 94.33 | 95.31 | 95.91 | 95.26 | 96.02 |

| Network | | Baseline | | DML | | | KDCL | | | MetaMixer (Ours) | | |
|-----------|------------|----------|-------|-------|-------|-------|-------|-------|--------------|------------------|--------------|--------------|
| Net 1 | Net 2 | Net 1 | Net 2 | Net 1 | Net 2 | Ens. | Net 1 | Net 2 | Ens. | Net 1 | Net 2 | Ens. |
| ResNet-20 | ResNet-32 | 69.38 | 71.10 | 70.37 | 72.49 | 73.52 | 70.60 | 72.84 | 73.96 | 71.96 | 74.83 | 75.17 |
| ResNet-56 | ResNet-110 | 72.88 | 74.14 | 74.03 | 75.82 | 76.67 | 74.30 | 75.92 | 77.28 | 76.67 | 78.77 | 79.63 |
| ResNet-32 | WRN-16-2 | 71.10 | 72.96 | 72.83 | 74.09 | 75.38 | 73.44 | 74.74 | 76.22 | 75.10 | 76.26 | 77.19 |
| WRN-16-2 | WRN-28-2 | 72.96 | 75.14 | 74.10 | 76.31 | 76.99 | 75.06 | 77.15 | 78.53 | 76.21 | 79.02 | 79.38 |
| WRN-16-2 | WRN-40-2 | 72.96 | 75.87 | 74.17 | 77.44 | 77.81 | 75.13 | 78.09 | 78.68 | 76.22 | 80.04 | 80.11 |
| VGG-13-BN | WRN-16-2 | 74.08 | 72.96 | 75.65 | 73.99 | 77.21 | 77.21 | 74.98 | 79.12 | 78.76 | 75.80 | 78.87 |

Table 2: Top-1 test accuracy (%) compared with various online distillation methods on CIFAR-10 (top) and CIFAR-100 (bottom) dataset by training two networks with different architectures. All the notations are the same as the ones in Table 1.

| Network | Baseline | DML | ONE | KDCL | MCL | MetaMixer (Ours) |
|-----------|----------|-------|-------|-------|--------------|------------------|
| ResNet-18 | 69.72 | 69.88 | 70.14 | 69.83 | <u>70.32</u> | 70.88 |

Table 3: Top-1 test accuracy (%) compared with various online distillation methods on ImageNet by training two networks with the same architecture. The result of MCL is from the original paper [38]. Reported the average performance of 3 runs.

ResNet (WRN) [42], VGG [29], and ShuffleNetV2 [23] on benchmark datasets including CIFAR-10/100 [16] and ImageNet [5]. For the VGG experiments, we use VGG models with batch normalization. For the efficiency of distillation, instead of training from scratch, we separately pre-trained the student networks using cross-entropy loss on the target dataset as the baseline and transferred the weights for the online distillation.

For CIFAR-10/100 experiments, we train each network for 160 epochs with a batch size of 128. We used stochastic gradient descent (SGD) optimizers with a momentum of 0.9 and a weight decay rate of 5×10^{-4} . The initial learning rate of optimizers is set to 0.05, and it is multiplied by 0.1 at the 40th, 70th, 100th, and 130th epoch. We warm up all distillation loss linearly from 0 for 20 epochs. The temperature of logit distillation is set to be 4, while we find that a temperature of 3 also works well.

For ImageNet experiments, we train each student network for 100 epochs with a batch size of 256. We also use SGD optimizers with a momentum of 0.9 and a weight decay of 1×10^{-4} . The initial learning rate is set to 0.02, and it is divided by 10 at the 10th, 40th, and 70th epoch. For the training data augmentation, we follow the standard data augmentation strategy as described in [17]. For the test phase, images are resized to 256×256 and then center-cropped to 224×224 . The temperature of logit distillation is set to be 4.

We compared our proposed method with several state-of-the-art online KD methods, including DML [44], ONE [18], KDCL [7], and MCL [38]. As ONE is configured to share low-level layers for different network branches, in our experiment, we treat different branches of ONE as different networks. For a fair comparison, all of the experimental results are the average over three runs, and we rounded the results to two decimal places. Besides measuring the performance of each student network, we also measure the ensemble performance of the student models by averaging their predictions.

4.2. Main Results

4.2.1 Results on CIFAR-10/100

We mainly evaluated the performance of our proposed MetaMixer on CIFAR-10/100 dataset with two student networks, while the performance with more student networks

is available in our ablation study in section 4.3.2. For MetaMixer, since the network structure of student networks is not necessarily identical, we classified our experiments into two categories: student networks with the same structure and student networks with different structures. For the experiments where the student models are of different architectures, we tried several representative combinations of models, including models of different depth/capacity, and models of different types.

Same architecture. From the experimental results in Table 1, we find that MetaMixer consistently outperforms the state-of-the-art online KD methods on both CIFAR-10 and CIFAR-100 in terms of average performance and ensemble performance. Besides the improved performance, on CIFAR-100, we find an interesting phenomenon that compared with other methods which tend to have a fixed performance gain over the baseline, the performance gain of MetaMixer increases steadily with deeper and larger models, and we will investigate this feature in the ablation study in section 4.3.3.

Different architectures. In this experiment, we validate the capability of different methods in dealing with model peers of different structures and model capacities. The results of ONE and MCL are not presented for models with different architectures. This is because ONE cannot be applied when two networks are of different architectures due to the configuration of sharing the low-level layers. Also, as MCL takes the advantage of contrastive learning mechanism, the performance of MCL gets greatly negatively affected with models of different capacities.

As indicated in Table 2, when the models are of different architectures, the performance advantage of MetaMixer over other online KD approaches is still significant both in terms of the average performance and the ensemble performance.

4.2.2 Results on ImageNet

We also evaluated the performance of MetaMixer on the ImageNet dataset which is much larger than CIFAR-10/100. We trained two peer networks of the same structure mutually with different methods and analyzed the mean performance of the two networks, as shown in Table 3. Our experimental result shows that the MetaMixer outperforms all of the online KD methods, which validates the effectiveness

| Network | Baseline | Without mixing | | Global Only | | Local Only | | MetaMixer | |
|-----------|----------|----------------|-------|-------------|-------|------------|-------|-----------|-------|
| | | Avg. | Ens. | Avg. | Ens. | Avg. | Ens. | Avg. | Ens. |
| ResNet-32 | 71.10 | 72.91 | 74.86 | 73.68 | 75.39 | 74.54 | 76.43 | 74.79 | 76.45 |
| ResNet-56 | 72.88 | 74.75 | 76.83 | 75.21 | 77.38 | 76.72 | 78.62 | 76.93 | 78.70 |
| WRN-16-2 | 72.96 | 74.52 | 76.25 | 75.14 | 76.73 | 76.09 | 77.94 | 76.40 | 77.88 |

Table 4: Top-1 test accuracy (%) comparison on CIFAR-100 by mutually training two networks of the same structure with different mixing stages of MetaMixer.

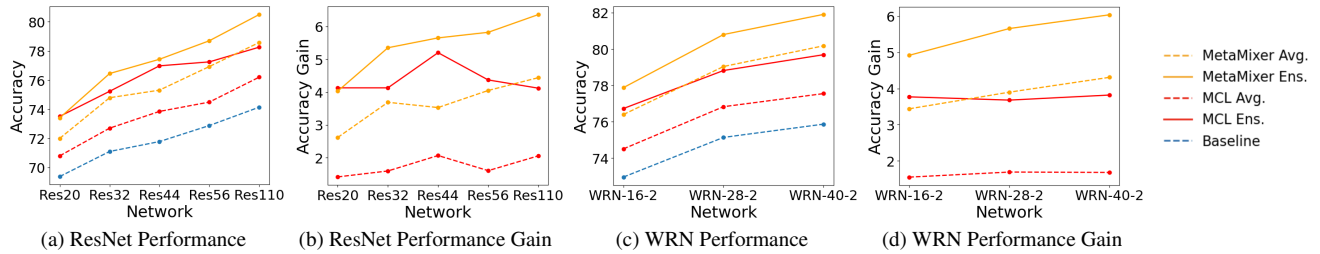


Figure 2: The performance and performance gain of mutually training two ResNet or Wide ResNet models with the same structure of different model depth and network capacity on CIFAR-100 dataset. From the result, we can see that compared with MCL which tends to have a fixed performance gain, the performance gain of our method increases steadily with the increase of network depth and capacity.

of our methods on the large-scale dataset.

4.3. Ablation Studies and Analyses

4.3.1 Effect of Different Mixing Stages in MetaMixer

Our proposed MetaMixer contains two consecutive mixing stages, which are local mixing and global mixing. In this ablation study, we investigate the effect of different mixing stages by training two networks with different mixing stages on CIFAR-100. From the experimental result in Table 4, we can see that either global mixing or local mixing can improve the average and ensemble performance, and the combination of local and global mixing can provide further performance gain in terms of average accuracy. Interestingly, during this ablation study, we found that the ensemble performance of networks trained only with the local mixing can be sometimes comparable with the ensemble performance of MetaMixer, leaving it an interesting point worth further investigating.

4.3.2 Performance with Multiple Student Networks

To further evaluate the effectiveness of our proposed method, we generalized our online KD method to multiple student networks to evaluate the performance. Specifically, we jointly trained multiple networks with the same architecture on CIFAR-100 dataset and evaluated the average per-

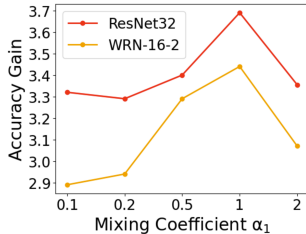
| Network | 2 models | | 3 models | | 4 models | |
|---------|----------|-------|----------|-------|----------|-------|
| | Avg. | Ens. | Avg. | Ens. | Avg. | Ens. |
| Res-32 | 74.79 | 76.45 | 74.91 | 77.69 | 74.92 | 77.54 |
| Res-56 | 76.93 | 78.70 | 76.93 | 79.66 | 76.91 | 79.64 |
| W-16-2 | 76.40 | 77.88 | 76.48 | 79.02 | 76.39 | 78.66 |

Table 5: Top-1 test accuracy (%) of mutually training multiple networks with the same architecture on CIFAR-100 dataset using MetaMixer.

formance along with the ensemble performance. As shown in Table 5, when the size of the student cohort increases from two to three, the average performance improvement is small compared with the two-model case. However, we witness a significant improvement in the ensemble performance. Also, we find that both the average and the ensemble performance saturate at three models.

4.3.3 Performance Gain vs. Network Capacity

Experiments were also conducted to evaluate the performance gain of our method with the increase of network depth and capacity. In this experiment, we use ResNet and Wide ResNet series on the CIFAR-100 dataset. We jointly



(a) Performance gain when $\alpha_2 = 0.2$ (b) Performance gain when $\alpha_1 = 1$

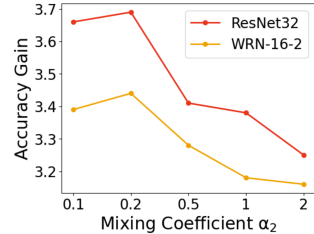


Figure 3: The impact of α_1 and α_2 on the average performance gain on CIFAR-100. As shown in the figure, the best performance is achieved with $\alpha_1 = 1$ and $\alpha_2 = 0.2$.

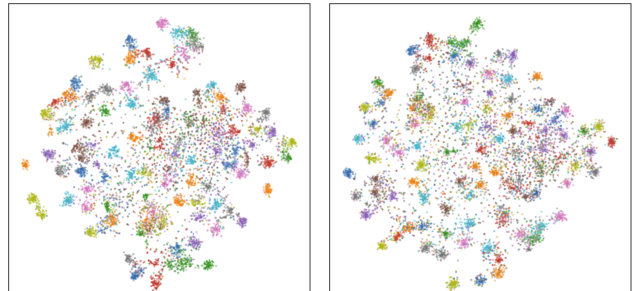
train two networks with the same architecture and compared the performance gain of MetaMixer with other different online KD methods. As shown in Fig. 2, different from MCL which tends to have a fixed performance gain, the average and ensemble performance gain of MetaMixer increases steadily with the increase of network depth and capacity. We believe this is a feature helpful for training larger models. We hypothesize that the reason behind this might be that MetaMixer, as a regularization strategy, can augment meaningful samples in the training process to avoid overfitting, while other methods like MCL and KDCL focus on designing better supervision for the student network and have nothing to do with regularization and overfitting issue. With the overfitting issue alleviated, larger models can benefit more from extra parameters and generalize better.

4.3.4 Ablation of Mixing Coefficient λ_1 and λ_2

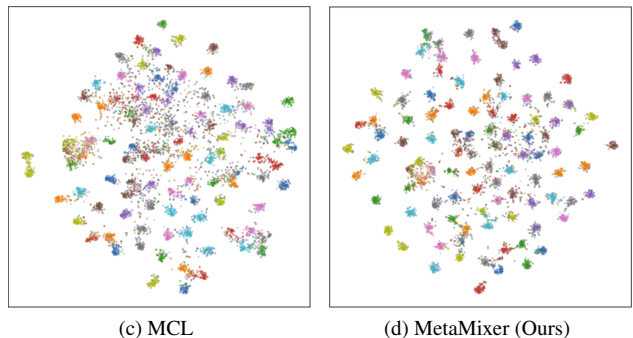
In MetaMixer, there are two different mixing stages: local mixing and global mixing. Thus, two different mixing coefficients λ_1 and λ_2 as described in Eq. 1 and Eq. 2 are introduced into our method. As indicated above, both of the mixing coefficients are sampled from beta distributions where $\lambda_1 \sim Beta(\alpha_1, \alpha_1)$ and $\lambda_2 \sim Beta(\alpha_2, \alpha_2)$. In this ablation, we evaluated the performance of MetaMixer with $\alpha_1, \alpha_2 \in \{0.1, 0.2, 0.5, 1, 2\}$ and searched the best combination of α_1 and α_2 on the CIFAR-100 dataset using two networks with the same structure. We measured the average performance gain under different combinations of α_1 and α_2 as shown in Fig. 3. The best performance is achieved with $\alpha_1 = 1$ and $\alpha_2 = 0.2$.

4.3.5 T-SNE Visualization

In this experiment, we present the t-SNE [32] visualization of the embedding space generated by models trained with different online KD methods. Specifically, we mutually



(a) DML (b) KDCL



(c) MCL (d) MetaMixer (Ours)

Figure 4: T-SNE visualization of embedding spaces generated by ResNet-110 models trained with different online KD methods on CIFAR-100. The figure shows that the model trained with MetaMixer can produce feature representations that are more separable compared with models trained with other online KD methods.

trained two ResNet-110 networks on CIFAR-100 with different online KD methods including DML, KDCL, MCL, and MetaMixer. As shown in Fig. 4, the experimental result shows that the embedding space produced by models trained with the MetaMixer is more separable than those trained with other online KD methods.

5. Conclusion

In this paper, we present a novel perspective on online KD through a regularization strategy that involves a two-stage mixing operation. More importantly, we highlight the limitation of existing online KD methods, which mainly concentrate on improving the distillation of high-level knowledge such as probability distribution, while neglecting the value of low-level knowledge in collaborative learning. In contrast, MetaMixer integrates knowledge from multiple scales and achieves significant improvements over the state-of-the-art online KD methods on representative benchmark datasets. We hope our work can foster future research on online KD and collaborative learning.

References

[1] Cristian Buciluă, Rich Caruana, and Alexandru Niculescu-Mizil. Model compression. In *Proceedings of the 12th ACM SIGKDD International Conference on Knowledge Discovery and Data Mining*, pages 535–541, 2006. [1](#)

[2] Defang Chen, Jian-Ping Mei, Can Wang, Yan Feng, and Chun Chen. Online knowledge distillation with diverse peers. In *Proceedings of the AAAI Conference on Artificial Intelligence*, volume 34, pages 3430–3437, 2020. [1](#)

[3] Jang Hyun Cho and Bharath Hariharan. On the efficacy of knowledge distillation. In *Proceedings of the IEEE/CVF International Conference on Computer Vision*, pages 4794–4802, 2019. [1](#)

[4] Inseop Chung, SeongUk Park, Jangho Kim, and Nojun Kwak. Feature-map-level online adversarial knowledge distillation. In *International Conference on Machine Learning*, pages 2006–2015, 2020. [1, 2](#)

[5] Jia Deng, Wei Dong, Richard Socher, Li-Jia Li, Kai Li, and Li Fei-Fei. Imagenet: A large-scale hierarchical image database. In *2009 IEEE Conference on Computer Vision and Pattern Recognition*, pages 248–255, 2009. [6](#)

[6] Ross Girshick. Fast r-cnn. In *Proceedings of the IEEE International Conference on Computer Vision*, pages 1440–1448, 2015. [1](#)

[7] Qiushan Guo, Xinjiang Wang, Yichao Wu, Zhipeng Yu, Ding Liang, Xiaolin Hu, and Ping Luo. Online knowledge distillation via collaborative learning. In *Proceedings of the IEEE/CVF Conference on Computer Vision and Pattern Recognition*, pages 11020–11029, 2020. [1, 2, 6](#)

[8] Song Han, Huizi Mao, and William J Dally. Deep compression: Compressing deep neural networks with pruning, trained quantization and huffman coding. *arXiv preprint arXiv:1510.00149*, 2015. [1](#)

[9] Kaiming He, Georgia Gkioxari, Piotr Dollár, and Ross Girshick. Mask r-cnn. In *Proceedings of the IEEE International Conference on Computer Vision*, pages 2961–2969, 2017. [1](#)

[10] Kaiming He, Xiangyu Zhang, Shaoqing Ren, and Jian Sun. Deep residual learning for image recognition. In *Proceedings of the IEEE Conference on Computer Vision and Pattern Recognition*, pages 770–778, 2016. [1, 4](#)

[11] Byeongho Heo, Jeesoo Kim, Sangdoo Yun, Hyojin Park, Nojun Kwak, and Jin Young Choi. A comprehensive overhaul of feature distillation. In *Proceedings of the IEEE/CVF International Conference on Computer Vision*, pages 1921–1930, 2019. [1](#)

[12] Byeongho Heo, Minsik Lee, Sangdoo Yun, and Jin Young Choi. Knowledge transfer via distillation of activation boundaries formed by hidden neurons. In *Proceedings of the AAAI Conference on Artificial Intelligence*, volume 33, pages 3779–3787, 2019. [1](#)

[13] Geoffrey Hinton, Oriol Vinyals, and Jeff Dean. Distilling the knowledge in a neural network. *arXiv preprint arXiv:1503.02531*, 2015. [1, 2, 4](#)

[14] Andrew G Howard, Menglong Zhu, Bo Chen, Dmitry Kalenichenko, Weijun Wang, Tobias Weyand, Marco Andreetto, and Hartwig Adam. Mobilenets: Efficient convolutional neural networks for mobile vision applications. *arXiv preprint arXiv:1704.04861*, 2017. [1](#)

[15] Zehao Huang and Naiyan Wang. Like what you like: Knowledge distill via neuron selectivity transfer. *arXiv preprint arXiv:1707.01219*, 2017. [2](#)

[16] Alex Krizhevsky and Geoffrey Hinton. Learning multiple layers of features from tiny images. 2009. [6](#)

[17] Alex Krizhevsky, Ilya Sutskever, and Geoffrey E Hinton. Imagenet classification with deep convolutional neural networks. *Communications of the ACM*, 60(6):84–90, 2017. [1, 6](#)

[18] Xu Lan, Xiatian Zhu, and Shaogang Gong. Knowledge distillation by on-the-fly native ensemble. *Advances in Neural Information Processing Systems*, 31, 2018. [1, 2, 6](#)

[19] Chengcheng Li, Zi Wang, and Hairong Qi. Online knowledge distillation by temporal-spatial boosting. In *Proceedings of the IEEE/CVF Winter Conference on Applications of Computer Vision*, pages 197–206, 2022. [1, 2](#)

[20] Hao Li, Asim Kadav, Igor Durdanovic, Hanan Samet, and Hans Peter Graf. Pruning filters for efficient convnets. *arXiv preprint arXiv:1608.08710*, 2016. [1](#)

[21] Yawei Li, Shuhang Gu, Luc Van Gool, and Radu Timofte. Learning filter basis for convolutional neural network compression. In *Proceedings of the IEEE/CVF International Conference on Computer Vision*, pages 5623–5632, 2019. [1](#)

[22] Jonathan Long, Evan Shelhamer, and Trevor Darrell. Fully convolutional networks for semantic segmentation. In *Proceedings of the IEEE Conference on Computer Vision and Pattern Recognition*, pages 3431–3440, 2015. [1](#)

[23] Ningning Ma, Xiangyu Zhang, Hai-Tao Zheng, and Jian Sun. Shufflenet v2: Practical guidelines for efficient cnn architecture design. In *Proceedings of the European Conference on Computer Vision (ECCV)*, pages 116–131, 2018. [6](#)

[24] Seyed Iman Mirzadeh, Mehrdad Farajtabar, Ang Li, Nir Levine, Akihiro Matsukawa, and Hassan Ghasemzadeh. Improved knowledge distillation via teacher assistant. In *Proceedings of the AAAI Conference on Artificial Intelligence*, volume 34, pages 5191–5198, 2020. [1](#)

[25] Pavlo Molchanov, Stephen Tyree, Tero Karras, Timo Aila, and Jan Kautz. Pruning convolutional neural networks for resource efficient inference. *arXiv preprint arXiv:1611.06440*, 2016. [1](#)

[26] Wonpyo Park, Dongju Kim, Yan Lu, and Minsu Cho. Relational knowledge distillation. In *Proceedings of the IEEE/CVF Conference on Computer Vision and Pattern Recognition*, pages 3967–3976, 2019. [2](#)

[27] Baoyun Peng, Xiao Jin, Jiaheng Liu, Dongsheng Li, Yichao Wu, Yu Liu, Shunfeng Zhou, and Zhaoning Zhang. Correlation congruence for knowledge distillation. In *Proceedings of the IEEE/CVF International Conference on Computer Vision*, pages 5007–5016, 2019. [2](#)

[28] Adriana Romero, Nicolas Ballas, Samira Ebrahimi Kahou, Antoine Chassang, Carlo Gatta, and Yoshua Bengio. Fitnets: Hints for thin deep nets. *arXiv preprint arXiv:1412.6550*, 2014. [1, 2, 4](#)

[29] Karen Simonyan and Andrew Zisserman. Very deep convolutional networks for large-scale image recognition. *arXiv preprint arXiv:1409.1556*, 2014. [1, 6](#)

[30] Yonglong Tian, Dilip Krishnan, and Phillip Isola. Contrastive representation distillation. *arXiv preprint arXiv:1910.10699*, 2019. 2

[31] Frederick Tung and Greg Mori. Similarity-preserving knowledge distillation. In *Proceedings of the IEEE/CVF International Conference on Computer Vision*, pages 1365–1374, 2019. 2

[32] Laurens Van der Maaten and Geoffrey Hinton. Visualizing data using t-sne. *Journal of Machine Learning Research*, 9(11), 2008. 8

[33] Vikas Verma, Alex Lamb, Christopher Beckham, Amir Najaifi, Ioannis Mitliagkas, David Lopez-Paz, and Yoshua Bengio. Manifold mixup: Better representations by interpolating hidden states. In *International Conference on Machine Learning*, pages 6438–6447, 2019. 3

[34] Dongdong Wang, Yandong Li, Liqiang Wang, and Boqing Gong. Neural networks are more productive teachers than human raters: Active mixup for data-efficient knowledge distillation from a blackbox model. In *Proceedings of the IEEE/CVF Conference on Computer Vision and Pattern Recognition*, pages 1498–1507, 2020. 3

[35] Kuan Wang, Zhijian Liu, Yujun Lin, Ji Lin, and Song Han. Haq: Hardware-aware automated quantization with mixed precision. In *Proceedings of the IEEE/CVF Conference on Computer Vision and Pattern Recognition*, pages 8612–8620, 2019. 1

[36] Zi Wang, Chengcheng Li, and Xiangyang Wang. Convolutional neural network pruning with structural redundancy reduction. In *Proceedings of the IEEE/CVF Conference on Computer Vision and Pattern Recognition*, pages 14913–14922, 2021. 1

[37] Guile Wu and Shaogang Gong. Peer collaborative learning for online knowledge distillation. In *Proceedings of the AAAI Conference on Artificial Intelligence*, volume 35, pages 10302–10310, 2021. 1

[38] Chuanguang Yang, Zhulin An, Linhang Cai, and Yongjun Xu. Mutual contrastive learning for visual representation learning. In *Proceedings of the AAAI Conference on Artificial Intelligence*, volume 36, pages 3045–3053, 2022. 2, 6

[39] Li Yuan, Francis EH Tay, Guilin Li, Tao Wang, and Jiashi Feng. Revisiting knowledge distillation via label smoothing regularization. In *Proceedings of the IEEE/CVF Conference on Computer Vision and Pattern Recognition*, pages 3903–3911, 2020. 1

[40] Sangdoo Yun, Dongyoon Han, Seong Joon Oh, Sanghyuk Chun, Junsuk Choe, and Youngjoon Yoo. Cutmix: Regularization strategy to train strong classifiers with localizable features. In *Proceedings of the IEEE/CVF International Conference on Computer Vision*, pages 6023–6032, 2019. 3

[41] Sergey Zagoruyko and Nikos Komodakis. Paying more attention to attention: Improving the performance of convolutional neural networks via attention transfer. *arXiv preprint arXiv:1612.03928*, 2016. 1

[42] Sergey Zagoruyko and Nikos Komodakis. Wide residual networks. *arXiv preprint arXiv:1605.07146*, 2016. 6

[43] Hongyi Zhang, Moustapha Cisse, Yann N Dauphin, and David Lopez-Paz. mixup: Beyond empirical risk minimization. *arXiv preprint arXiv:1710.09412*, 2017. 3

[44] Ying Zhang, Tao Xiang, Timothy M Hospedales, and Huchuan Lu. Deep mutual learning. In *Proceedings of the IEEE Conference on Computer Vision and Pattern Recognition*, pages 4320–4328, 2018. 1, 2, 6

[45] Borui Zhao, Quan Cui, Renjie Song, Yiyu Qiu, and Jiajun Liang. Decoupled knowledge distillation. In *Proceedings of the IEEE/CVF Conference on Computer Vision and Pattern Recognition*, pages 11953–11962, 2022. 1

[46] Hengshuang Zhao, Jianping Shi, Xiaojuan Qi, Xiaogang Wang, and Jiaya Jia. Pyramid scene parsing network. In *Proceedings of the IEEE Conference on Computer Vision and Pattern Recognition*, pages 2881–2890, 2017. 1